



GLOBAL JOURNAL OF RESEARCHES IN ENGINEERING: J
GENERAL ENGINEERING
Volume 24 Issue 1 Version 1.0 Year 2024
Type: Double Blind Peer Reviewed International Research Journal
Publisher: Global Journals
Online ISSN: 2249-4596 & Print ISSN: 0975-5861

New Ability for Analysis of the Focus Zone of the Crust Seismic Events

By Alexey G. Epiphansky

Abstract- The initial goal of this work was to improve the location algorithms used to determine the depth of crustal events. Eventually, it became apparent that we were incapable of determining the depth of what is required. The location problem has solutions based on Geiger methods. Iteration procedures are used to solve this mathematical task that is purely mathematical. The mean square residual is the criteria used to conclude the iteration procedure. The physical problem of estimating the origin location and impact of the following earthquake on surrounding environments has not been addressed by any of them. It's clear that the impact is dependent on radiation during seismic activity.

From the other side, the beginning of the seismic events is determined by the set of arrival times, which is the sole instrumental evidence of the process. So it is clear that having kinematic parameters, such as arrival times, is necessary to determine a dynamic solution. Sure, the seismic records are available for use.

Keywords: seismic events location, event depth, focal zone, seismic depth phases, rupture line, characteristic lines, sub focuses.

GJRE-J Classification: LCC: QE534.2



Strictly as per the compliance and regulations of:



New Ability for Analysis of the Focal Zone of the Crust Seismic Events

Alexey G. Epiphansky

Abstract- The initial goal of this work was to improve the location algorithms used to determine the depth of crustal events. Eventually, it became apparent that we were incapable of determining the depth of what is required. The location problem has solutions based on Geiger methods. Iteration procedures are used to solve this mathematical task that is purely mathematical. The mean square residual is the criteria used to conclude the iteration procedure. The physical problem of estimating the origin location and impact of the following earthquake on surrounding environments has not been addressed by any of them. It's clear that the impact is dependent on radiation during seismic activity.

From the other side, the beginning of the seismic events is determined by the set of arrival times, which is the sole instrumental evidence of the process. So it is clear that having kinematic parameters, such as arrival times, is necessary to determine a dynamic solution. Sure, the seismic records are available for use.

At this time, it has been recognized that a new algorithm is required to identify the location with the most seismic energy radiation. The first arrival times must be matched to this location. Secondly, the internal structure of a focus zone must be decomposed by seismic energy using the new algorithm. During the investigation it appears that travel time tables have self-organized structures.

These structures were called a "rupture line" which associates with the event itself and characteristics each of which associates with used seismic phases. In this work two seismic phases are used: phase P and phase pP . These structures became the basis of algorithms which are able to focus on any point that lies within the focus zone and translate dynamic parameters from seismic records into these points. Thus, formulated tasks are solved and the algorithms are derived. Some results demonstrate the data processing of the actual seismic events in conclusion of the article.

Keywords: seismic events location, event depth, focal zone, seismic depth phases, rupture line, characteristic lines, sub focuses.

I. INTRODUCTION

Earthquake focus location procedures and its applications had appeared long before the XIX century. Automated procedures and wide-scale use of it were appearing in the middle of the XX century. So it may seem that we should know all about location procedures itself and Earth interior, nothing new can be found in this way.

Nevertheless, it turned out – something new may be found at hand. Detailed analysis showed that

new is hidden in the velocity structure of the crust and upper mantle. It comes from here into generalized seismic travel tables fluently.

To be honest, this requires time, power computers, digital seismic records and time synchronization of seismic recorders.

The work is based on data processing of seismic records obtained from different agencies. Most seismological investigations deal with particular seismic events. In our case we have analyzed the process of location itself, and try to generalize the results to have as comprehensive as possible valuable algorithms.

We had been searching common intermediate appearances of some dependencies of the time delaying from depths when such dependencies were found. The object of investigation was changed at that moment: instead of location procedures the model of crust seismic events became the object of investigation.

At the same time, we meet with disagreement: the result of seismic event location is a point. For the earthquake appearance it is required that in its sources were presented the movements of a big¹ mass of material with varying acceleration. That generates enough kinetic energy to produce an observed action as an earthquake. This point gives a start to changing the direction of the investigation. We began searching for a way to describe the focal zone model in terms of energy.

Now, we can talk about the tools we used in this investigation. At first, we were using a standard location algorithm. This work uses a modified Geiger algorithm of location ([Geiger, L., 1912]), supplemented with the simplex method ([Ge, M., 1995]; [Prugger, A., et al., 1989]).

Work carried out in a frame of investigation of the ability to elaborate automated determination of the core events depth. Nevertheless, we were trying to find the ability to work terms energy².

II. RUPTURE LINE

Geiger method permits finding the location of most seismic events if they have enough arrivals starting from an arbitrary hypocentre approach. But almost near

¹ In the article [Bruno, J., 1968] it was shown that direct measurement of displacements in rupture zones are few cm per year. This small displacement required the simultaneous movements of a big mass of material.

² Energy could not be associated with a point, only for volume of material it may be done.

Author: Ph.D., Leading Engineer, Geophysical Survey of Russian Academy of Science, Obninsk, RF. e-mail: epiphansky@gmail.com

the final point of the solution the convergence began to decrease. To understand the reason that led to such behavior, the location algorithm was changed on the final steps. The Geiger method was changed by the simplex method which was combined with a fixed depth calculation procedure. This procedure consequently changes depth with fixed steps for each new hypocentre location.

The result showed that hypocentres were lining up to the chain. Analysis indicated that Chan's links form a smooth line. This effect was observed for all processed events. This line is located in 4D space: three 3D space coordinates and time. But only two of four coordinates have significant meaning – depth and time. This is a common property for any set of first arrivals of the same seismic event. We named this effect “rupture line”. It is not a line of rupture in reality. This line is the locus of hypocentres obtained by the location procedure.

Strictly speaking, a rupture line is a structure or object (from algorithmic points of view). An element of this structure involves several parameters. Each element corresponds to hypocentre location. Mathematically, it may be written as:

$$\mathcal{W}(h) = \{w = w(t_0, \varphi, \lambda, h; \mathcal{R})\}, \quad (1)$$

where $w()$ - a function that determines parameters of the structure elements. First four parameters determined hypocentre location. Fifth parameter \mathcal{R} is a mean square root residual (RMS). This parameter defines the quality of the location solution. We can write expressions for RMS as:

$$\mathcal{R}(\mathcal{E}, h) = \frac{1}{(M - n)} \sqrt{\sum_{m=1}^M \tau_m^2(h)}, \quad (2)$$

where $\mathcal{E} = (t_0, \varphi, \lambda)$ - epicentre parameters, h - a trail depth, τ_m - phase residual, $m(m = 1, \dots, M)$ - index of seismic phase, M - total phase number, n - number of independently defined parameters. Phase residual is:

$$\tau(r_m, h) = t_m - t_m^C(r_m, h) + \epsilon_m, \quad (3)$$

where τ - phase residual dependent of epicentral distance r_m and trail depth; t_m - observed time arrival of phase m , $t_m^C(r_m, h)$ - calculated time arrival for phase m which is dependent from epicentral distance and depth and may be obtained from travel time tables. The last summand ϵ_m - presents uncertainty of measurement of m 's time arrival. Uncertainty of the measurement should be present in expression of a phase residual, but it may be put to zero without loss of generality during formal expressions manipulations.

The calculated time arrival may written as $t_m^C(r_m, h) = t_0(h) + \gamma(r_m, h)$, where $t_0(h)$ - origin time, $\gamma(r_m, h)$ - a function to calculate time delaying by travel

time tables. Now we can write an expression for the first argument in (1):

$$t_0(h) = \langle (t_m^C - \gamma(r_m, h)) \rangle = \langle t_m^0(h) \rangle, \quad (4)$$

where argument in last term $t_m^0(h)$ -is a phase origin time, the angle brackets means the operator taking the average of the argument. As usual, algorithms that use the Geiger method or simplex technique are find a value of the origin time by averaging the middle term of expression (4). Expression (4) indicates dependencies between parameters from structures of different types – the first structure is a rupture line; next is discussed in the next section.

Fig. 1 presents the graphs of three coordinates of the rupture line – origin time (a), latitude (b) and longitude (c). Fourth coordinate - depth is a parameter (vertical axis). Two coordinates are parameters of the structure – origin time and depth. It means that any one of these parameters define location along this structure. The last indicates strong dependencies of these two parameters. That is vital for our further considerations. The presented result was obtained from the data processing of the event 2022.01.7 17:40:34 in China. It is essential that dependencies for space coordinates from depth are weak. This deviations from a straight vertical line originated by in homogeneity of media of propagation seismic waves and due to discrepancy Globe with ideal sphere form — deviation value in $1^\circ \cdot 10^{-5}$ (arc degree) corresponds to 1.19 m.

III. CHARACTERISTICS

The last term in expression (4) does not contain parameters of a rupture line. At the same time, the first term is rupture line parameters only.

This leads us to mind: maybe we have another linear structure similar but differs from the rupture line?

If in expression (4) we have structure in the left side and averaging operator of set of structure parameters in right, it quickly suggests that structures in argument in the right side have the similar behaviour to the structure in the left of (4).

For time arrivals can be written following expression:

$$t_m = t_0(h) + \gamma(r_m, h), \quad (5)$$

In the previous investigation³ was found: if $t_0(h) \in \mathcal{W}$ than $t_m = const$ for any h .

This assertion should be proven. But travel time tables obtained experimentally. So proving shall be based on comparing the results of data processing.

³ It was the same investigation where we met with the appearance of a rupture line structure.

Let us write the expression:

$$\mathcal{X}_m = \{t_m = t_0(h) + \gamma(r_m, h) \mid 0 \leq h < \Delta H \mid ; t_0(h) \in \mathcal{W}\}, \quad (6)$$

where $m = (1, \dots, M)$ is the number of the seismic records, ΔH - is a thickness of crust and upper mantle;

The expression (6) defines a mathematical set; let's call it a phase characteristic. Term phase means that we have such a set of t_m for each of the phases we are mentioned in the article. The set \mathcal{X}_m is similar to rupture line structure. The difference is that \mathcal{W} contains information from all arrival of the event, when each characteristic is connected only with one arrival.

Another similarity is that a characteristic element consists not only of parameter t_m , but of the following parameters $(t_m^0, h; t_m, a_m) \in \mathcal{X}_m$, where t_m^0 - a phase origin time, h - the depth along the characteristic, t_m - is arrival time, a_m - arrivals amplitude. The parameter t_m defines \mathcal{X}_m uniquely due to it being constant within characteristic. The params t_m^0 and h defines location along characteristic.

From (5), we can write

$$t_m^0(h) = t_m - \gamma(r_m, h). \quad (7)$$

This expression consists of absolute time in terms of $t_m^0(r_m, h)$ and t_m . To simplify comparing, we subtract $t_m^0(r, h)_{h=0}$ from both these terms (or from the left and right side of the expression (7)). Such a way, we got relative time expressions. It will be used later.

Now, we can compare the relative phase origin time values with the relative origin time values along the rupture line. We will be presented on a graph below the relative values of parameters only. We will be implied as a subtrahend parameter value on zero depth, if the opposite does not indicate.

Fig. 2 presente the dependence from depth of the origin time on a characteristic $t_m^0(r_m, h)$. Fig. 2.a are presented graphs for four epicentral distances. The epicentral distances are: line 1 - $r_m = 25^\circ$, line 2 - $r_m = 50^\circ$, line 3 - $r_m = 75^\circ$, line 4 - $r_m = 100^\circ$.

Fig. 2.b are presented graphs for the same epicentral distances, but as a subtrahend was taken the origin time at depth $h^f = 12.5 \text{ km}$. It is demonstrated that characteristics cross in one point corresponds to the focus depth. Fig. 2.c. presented comparing the dependence of a depth of the origin time on the characteristics and the origin time on the rupture time. Line 1 is the characteristic origin time with $r_m = 25^\circ$, line 2 is the characteristic origin time with $r_m = 100^\circ$; line 3 is the rupture line origin time. The results obtained for the event 2022-01-07 17:45:34 in China.

We can see on Fig. 2 that slope of a characteristic is changing with a changing of epicentral distance. Fig. 3 demonstrates in 3D projection two arguments function $\delta t(r, h) = t_0^x(r, h) - t_0^x(r, 0) = (\gamma(r, 0) - \gamma(r, h))$ which are obtained from (7) by eliminating absolute time.

We can see that the region of available epicentral distances splits into some zones. Two of them have smooth dependence on epicentral distances. This requires certain restrictions during the picking up of the seismic stations for data processing.

IV. LOCAL UNIT FOR MEASUREMENT OF ENERGY SIMILAR VALUES

The value of \mathcal{R} calculated along the rupture line might have not a minimum for some events in a reasonable interval of the depth. This does not mean that (2) is not working. It means that uncertainty of residuals in (3) in dependencies of the depth is large. Another reason may be unsuccessful selection of seismic stations. We will discuss this later. In this work we are very wide using this criteria \mathcal{R} for location procedure with fixed depth values. Coordinate location procedure finds out the minimum of value of \mathcal{R} always.

In this work, we will not concentrate on the problem of why the above might happen (see also [Dmitry Storchak, 2011] and [Engdahl, E.R., et al., 1998]). This is a well-known fact. This work suggests different criteria for the final solution. The suggestion is based on using a physical indicator. Such an indicator may be seismic energy (or value with similar properties) emission from the focal zone.

The final hypocentre is located on the rupture line in the point where seismic energy reaches maximal value. Actually, the rupture line is a locus of points of minimum expression (2) with fixed depth. This is coincidental with traditional location procedures. We are refusing to search the minimum of (2) by the depth and suggested searching the maximum of the energy radiations along the rupture line.

As an energy similar object, we are choosing the "amplitude parameter" or for short AmP . Its expression is

$$AmP = \frac{1}{M} \sum_{m=1}^M \left(\frac{1}{K} \sum_{k=1}^K \rho_m^2(f_k) \cdot f_k^2 \cdot \delta f \right) \quad (8)$$

where $\rho_m(f_k)$ - spectral amplitude, f_k - spectral frequency, δf - sampling interval, $k = (1, \dots, K)$ - frequency index, K - one side frequencies number of Fourier transforming (for positive and negative frequencies, it has the same value (see Appendix A)); $m = (1, \dots, M)$ - phase index and M - number of seismic records. AmP is calculated separately for each phase.

AmP has physical dimension $\left[\frac{m^2}{S^3} = \frac{m^2}{S^2} \cdot \frac{1}{S} \right]$. If AmP value multiply to granite density $\left(\rho = 2600 \frac{kg}{m^3} \right)$ on the Earth's surface, we will get dimension $\left[Nm \cdot \frac{1}{m^3 S} \right]$. So, the seismic radiation energy in Joules may be obtained by integration over the volume of the focus zone (this requires knowing how the energy radiation is distributed over the focal zone) and over the time of focus zone activity.

Desired algorithm was created. The algorithm is included another algorithm to calculate coherence in every point of the focus zone⁴. The last algorithm is a central part of described development. The vital ability of that algorithm is that it permits defining the main part of the spectral window. The main part is defined by the maximum coherence value. Appendix A describes it.

The AmP physical dimension is $\left[\frac{m^2}{S^3} \right]$. It is not an energy yet, but relations of two such values give us the same result as a relation of energy values. AmP may be used for comparing relation values instead energy in the frame of one event.

The first problem formulated in the frame of this work is a determination of the depth of crust events. The depth of the event may be determined by searching the maximum of seismic radiation along the rupture line. Unfortunately, we have an impenetrable obstacle – amplitude along characteristic is constant.

V. DEPTH PHASE pP

The determination of the event depth depends on the answer to the question: what is the depth of the seismic event? Traditionally, this parameter was taken from the mathematical solution of a location task. Unfortunately, this determination of term depth ignores physical aspects of earthquake phenomena.

This work suggested using depth value which corresponds to maximal radiation of seismic energy along rupture line. Considering, that amplitude along P characteristics are a constant it is possible to use another phase. The depth phase pP may be used instead of the P phase. pP phase has the same focus impulse⁵ as a phase P .

Fig. 4 shows the graphs of pP characteristics phase origin time in dependency of depth - continues lines and from epicentral distances – separated lines. The essential property of pP characteristics is that its derivative of phase origin time by depth is negative while P phase origin time derivative is positive. These two types of characteristics are crossing in a compact area

of 4D space. Later, we will examine this phenomenon in detail.

Before the next step, we rewrite expression (7) to make it clearer to which phase we mean

$$t_m^{0,pn}(h) = t_m^{pn} - \gamma^{pn}(r_m, h), \quad (7')$$

where pn is the seismic phase name: P or pP .

The result of the location procedure is presented in Fig. 5. This result was obtained from processing of the data of the event 2022-01-07 17:45:34 in China. That is an example of using both seismic phases P and pP . Fig. 5 presents three graphs of AmP : curve 1 - graph of $AmP^{(P)}$, curve 2 - graph of $AmP^{(pP)}$, curve 3 - graph of expression.

$$A_n = AmP_n^{(pP)} \cdot \left(\frac{\sum_{n=1}^N AmP_n^{(P)}}{\sum_{n=1}^N AmP_n^{(pP)}} \right) \quad (9)$$

where $n = (1, \dots, N)$ – index along rupture line and N – number of points where AmP was calculated; the value A_n is the reproduction of the values of $AmP^{(P)}$ by scaling $AmP^{(pP)}$. Thus, we are taking into account the difference in amplitude of vertical components⁶ of a direct wave (P phase) and a reflected wave (pP phase). Thus, we are bypath restrictions connected with the property of the P characteristics. Expression (9) presents the algorithm of amplitude coordinations.

The maximum on the curves 1 and 3 define depth value $h = 14.75 \text{ km}$, while USGS defined depth for this event as 13 km .

So, we see that developed algorithms are working. Let us now clarify how it works.

VI. THE SOLUTION SPACE AND FRAME REFERENCE

The schematic chart in Fig. 6 shows the collaboration of two dedicated seismic phases. First, we consider the frame reference of our solution. It is not a pure physical frame reference. 3D physical space will stay without changes. The fourth axis is a time. Chart in Fig. 6 is a slice of 4D space by a time-depth plane⁷. Line (A, B) and its continuation is the time axis. The line (A, C) and its continuation is P characteristic; the line (B, C) and its continuation is pP characteristic. It is drawn only one pair of characteristics belonging to the same record: we suggest that each recorder registered a pair of arrivals⁸ which can be detected as phases P and pP . We are assuming that two seismic phases always exist

⁴ The coherence is the normalized module of the complex sum of spectrum phases of the Fourier transforming of the focus impulses while spectrum amplitudes are ignored.

⁵ The term focus impulse is applied to a displacement or to an energy parameter. The meaning of this term is the same: one side finite smooth function.

⁶ We are using vertical components of the seismic records only.

⁷ The rupture line is a 4D curve. The deviations from the strict vertical line of the latitude and longitude values are relatively small. It can neglect these.

⁸ The recorder is registered for both seismic phases, but the standard detector does not detect both.

and therefore two characteristics exist too. The point C is a place where these two characteristics are crossing. According to the property of characteristics, the AmP along each of them are constant. What is the AmP value in point C ? It looks like we have a contradiction.

In reality, The source is located at the point C . The seismic radiation reaches the recorders with different amplitudes due to differences of the travel ways including radiation pattern. Hence, AmP^P does not equal to AmP^{PP} .

There are two solutions to the mentioned problem that are presented in this work. One was demonstrated in connection with location procedure. Second will be considered later.

Each element of characteristics contains both parameters: t_m^0 and t_m . First is the parameter which defines location along characteristic, second is a constant along characteristic. Value of event origin time t_0 is the averaging value of all characteristic parameters $t_m^0 (m = 1, \dots, M)$.

Let us segment (A, C) or (B, C) are the generalized characteristics: point A will be an origin time of phase P ; point B will be an origin time of phase pP . Point C is a place of crossing of both characteristics.

Let us introduce the value h^f as a fixed value of the focus depth. Another meaning of the parameter h^f is a focus depth. This (A, C) segment may be a characteristic of phase P or a rupture line.

In this case, $t_m^0(h^f) \equiv t_0(h^f) \forall m = (1, \dots, M)$ It means all characteristics and the rupture line are crossing at the point $(t_0(h^f), h^f)$ in 4D space.

Let us named of abscissa axis (time axis) as τ . In this case, we can write for point A expression $\tau_A = t_A^{0,P}(h)_{h=0} - t_0^P(h)_{h=0}$. The same expression we can write for point B $\tau_B = t_B^{0,pP}(h)_{h=0} - t_0^{pP}(h)_{h=0}$. According to (7) and to the fact that $\gamma^P(r, h)_{h=0} \equiv \gamma^{pP}(r, h)_{h=0}$ we have $\tau_A(h)_{h=0} \equiv \tau_B(h)_{h=0}$ If $h^f = 0$ then $\tau_A = \tau_B$. With depth increase the point B will be moved from τ_A point to the right.

We can write for τ next:
 $\tau_A = \gamma^P(h) - \gamma^P(h)_{h=0} < 0$ and $\tau_B = \gamma^{pP}(h) - \gamma^{pP}(h)_{h=0} > 0$.
 It easy to see that the distance of time between values τ_B and τ_A for depth $h = h^f$ is

$$\tau_B - \tau_A = \gamma^{pP}(h^f) - \gamma^P(h^f). \quad (10)$$

The expression (10) is essential for our following consideration. We can formally use (10) to define the depth at the point C by the difference between the time τ_A and τ_B

The solution frame reference consists of the 3D physical space and relative time.

VII. APPLYING DERIVED MATHEMATICAL INSTRUMENT FOR INVESTIGATION OF THE SEISMIC EVENTS FOCAL ZONE

This work was intended to improve depth location only. Eventually, we understood that our focus model should be improved too. Above, we described the procedure of determining events depth by applying amplitude parameters. The expression (9) converts the value of the $AmP^{PP}(h)$ into a $AmP(h)$. The last corresponds to the intensity of P phase. Thus, the new location algorithm was preserved to be close to the traditional one. Graphs on Fig. 5 show the level of seismic radiations along the rupture line. The last was obtained by data processing of an event's records.

The next step was an attempt to apply an amplitude parameter for generalizing the station's seismic records. It shows the relative radiation intensity for active (coseismic) time period. It shows that the curve of the seismic activity has one maximum impulse and several impulses of less intensity. The less intensity impulses are the appearance of an internal sub-focus. The last achievement is ability to plot distribution of the intensity of inner sub-foci. All this expansion was derived on the basis of mathematics described above.

The basis of algorithms is described above triangle A, B, C (Fig. 6). The line (A, C) is a part of the rupture line. Rupture line depends on the event's origin time, which depends on arrival times. If we forget about arrival times and will be changing origin time our geometrical construction that involves M triangles will be moving along a time axis as a single object (m is a number of recorders). In this case, inverse recalculations of new arrival times give the ability to take the amplitude parameters for new origin time. Thus, we can move along the time axis. The 3D space movement may be done by similar procedure.

It is possible to use all properties of the rupture line and all characteristics in the new time and space position. We can do it due to the fact that the parameters of our geometrical construction depend on the permanent data only.

Let us repeat the vital property: *the value of parameters of the characteristic element are constant*. According to this, the value of the AmP parameter on characteristic for depth zero will be translated to point C . We considered it early.

At the point C we have two AmP values. The problem is: how is it possible to agree on these two values? We used the following expression:

$$A = \frac{\sum_{m=1}^M (AmP_m^P \cdot AmP_m^{pP})}{\sum_{m=1}^M (AmP_m^P + 0.25AmP_m^{pP})}, \quad (11)$$

where A - resulting amplitude parameter value for each point on choosing subspace, $m = (1, \dots, M)$ - index of the seismic records, M -number of records. That is another variant of the algorithm of amplitude coordinations. First was presented as expression(9).

We point out that expression (11) gives out A in relative values. Usually, nobody uses energy in seismology, but it uses magnitudes. The last is relative value too. So it is not a problem to convert AmP to correspondent magnitude. In future we are planning for practical usage of such conversation. At the moment it is not important.

VIII. AN ADDITIONAL PART OF RESIDUAL VALUE DUE TO CHARACTERISTICS DEPENDENCES

The characteristics are crossing (Fig. 2.b) at one point if the uncertainty is zero. If $\epsilon \neq 0$ then correspondent characteristic will be shifted. This leads to shifting a cross point of some characteristics. As a result, the non zero value of ϵ influences indirectly onto a RMSI value of the event.

These uncertainty values are playing a complicated role in the averaging operator. Any error in arrival time causes characteristic's disagreement – error in arrival time shifts characteristic cross point along the rupture line. Instead of one cross point we have several shifts by depth. It is not possible to eliminate but it needs to be known.

The point of the crossing of the pair of characteristics are dependents from time and depth as it was shown above. Moreover, characteristics have different slopes by time (or by depth). This slope is dependent from the epicenter distances.

The Fig. 7 demonstrates the maximal of a deviation. As we can see, the deviation may reach seconds: the difference between $t_m^{0,(P)}(r, h)_{r=25, h=0}$ and $t_m^{0,(P)}(r, h)_{r=175, h=0}$ may reach 0.8 sec. For phase pP it is near the same. This is corresponds to the focus depth $h = 40 \text{ km}$. These estimations were made when the set of stations was restricted by teleseismic distances.

IX. EXAMPLES OF ACTUAL DATA PROCESSING BY THE DERIVED MATHEMATICAL TOOLS

It is commonplace to treat a model of the focus zone as a set of sub-foci. The evidence of each sub-focu is a focus impulse that is present in the seismic records. We are not meaning the displacements in the source. We are talking about evidence of the rise of seismic energy.

The impulse has two markable points in regard to Fig. 6: the beginning is the τ_A mark and an amplitude maximum the τ_B . Why are we connecting the maximum of the radiation with point B on Fig. 6? Fig. 5 may clarify this.

Fig. 8 shows a plot for the event 2022-01-07 17:45:34 in China. The curve of Fig. 8 is $AmP(t)$ generalized parameter calculated for $h = 0$ along the timeline in time interval $t = (-5, \dots, 20) \text{ sec}$. (Term generalized means: $AmP(t) = \frac{1}{M}(\sum_{m=1}^M AmP_m^p(t, h))_{h=c}$, where M - number of used seismic records.)

This plot illustrates what was said above. There is one global pulse in general and several local pulses with small amplitudes. The graphs shown on Fig. 8 result from applying an algorithm derived from expression (8). And again, we can see one global pulse and several local pulses of sub-foci (see Fig. 5). Fig. 5 plots were drawn along a rupture line. The Fig. 8 graph is very close to the graph on Fig. 5. The difference is in abscise units: one has a time and another depth.

The active process begins before the first braking pickup algorithm registered first arrivals. Another feature is the presence of several local maxima on both graphs. We can treat that as evidence of several focuses presented in the focal zone.

In this work, we are demonstrating the results of processing two seismic events:

1. 2022-01-07 17:45:34 in China and
2. 2024-01-22 18:09:09 Border of Kyrgyzstan & China.

Additional information about these events is given in Table 1.

First event has a crust origin and is a moderately normal seismic event without special features. We are using it as a coaching event. Fig. 5, 8 and 9 show some abilities for analysis of evaluation of this event. Fig. 5 shows the results of location data processing. Fig. 8 presents an generalized AmP parameter in time interval $t = (-5, \dots, 20) \text{ sec}$. Fig. 9 presents a map on a horizontal slice that consists of the origin vicinity. Map demonstrates the distributions of seismic activity. It draws attention to itself that origin consists of few ruptures.

Second event has an origin depth at the bottom of crust ($h = 42.7 \text{ km}$). Fig. 10.a presents the result of location data processing. It is interesting that USGS gave a depth of 13 km for both these events. It looks like this depth was fixed during the location procedure. Other features: seismic energy began to emit before first arrival times were registered (see Fig. 10.b). It is significant in seismology when we are observing some kind of precursor.

Fig. 11 presents two-dimensional slices of 3D space containing the origin. One slice Fig. 11.a presents a map of the seismic activity in the origin vicinity.

Moreover, we can trace several seconds of seismic activity before origin time on the vertical slices in coordinates (R, h) in backward time perspective.. Axis R is a segment of arc on the surface (line (A, B) on map Fig.11. a), the R unit is arc degree. Axis h is depth in km . All what shows on Fig. 11 for demonstration only. It pays attention that all vertical slices correspond to

times before zero time on graph Fig. 11.b. This picture series shows the rising of the seismic activity in the origin vicinity from mantle to up.

In general, Investigation of particular events does not aim for this work. It is a topic for another article.

It is required to emphasize some differences in final results of events location. Especially, t_0 strongly depends from the depth according to the rupture line properties. Coordinates have less dependents but these dependencies are present.

ACKNOWLEDGMENT

This work and investigation itself could not be successful without the help of Dr. Irina Gabsatarova and

Dr. Inessa Socolova. I express my deep appreciation to their patient, attention during our discussions and for support with data picupping.

Seismic data was uploaded throw web-services iIRIS included next seismic networks (<http://ds.iris.edu/mda>): (1) II Global Seismograph Network – IRIS/IDA (Scripps Institution of Oceanography); (2) IU Global Seismograph Network IRIS/GSN (Albuquerque Seismological Laboratory/USGS).

I appreciate the ability to work for the Union Geophysical Survey of RAS. I express my appreciation to all my colleagues who help me in this long investigation.

Table 1

Time	Location	Depth	Depth by source	M	Region & Source
2022-01-07 17:45:31.832	37.573° N 101.435° E	14.62 km	13 km	6.6	Northern Qinghai, China. Source: USGS
2024-01-22 18:09:09.223	41.033° N 78.905° E	42.75 km	13 km	7	Border of Kyrgyzstan & China. Source: USGS

APPENDIX A

Coherence Level and Amplitude Parameter

Seismic records coexist with all of the seismic signals over the whole planet's crust. The difference is in amplitudes of signals. By shape all seismic signals are similar. To separate signals from different sources one can use differences in terms "similar" and "the same". It means that signal amplitudes are ignored.

Seismic signals differ by length and amplitude increasing in time. Two of these features are enough to separate different signal sources. This is used in microseismic investigations mostly. The method is based on the "comparing operator" applied to spectral phases (with unknown amplitude) of Fourier transformation of the signal's pulse. A comparing operator is applied for all available seismic records – stacking method. This may presents by expression

$$\Phi = \frac{1}{K} \sum_{k=1}^K \left(\frac{\text{mod}(\sum_{m=1}^M e^{i\varphi_m(f_k)} w_m)}{\sum_{m=1}^M w_m} \right),$$

where $\varphi_m(f_k)$ - spectral phase on frequency f_k , w_m - weight function, K - one side frequencies numbers of Fourier transformation, M - number of seismic records. Algorithm is using discrete Fourier transform.

Some clarification about "one side frequency number". Obviously, the Fourier transformation is symmetrical operator in range $-\infty \leq f \leq \infty$. Fortunately there were several rules (William T. Vetterling, at. al., 1988) that permitted operation of computation to

bring a simple one side numerical operator. ([Ge, M., 1995]; [Prugger, A., et al., 1989]). On the basis of it is the fact that the impulse of a seismic source is one side finite in time smooth function.

Value Φ can be used for checking whether two or more seismic impulses coincide. It may evidence with higher degree of probability that two seismic phases P and pP were emitted by one source. The algorithm derived from Φ expression may operate with signals which amplitudes less than noise level.

For each seismic event frequency-time window may be determined where the coherence level reaches the maximum. Time sampling period is critical for frequency-time window parameters.

REFERENCES RÉFÉRENCES REFERENCIAS

1. Brune, J. (1968). Seismic Moment, Seismicity, and Rate of Slip along Major Fault Zones. *J. Geophys. Res.*, v.73 v. 2, pp. 777 - 784.
2. Engdahl, E.R., van der Hilst, R. & Buland, R., (1998). Global teleseismic earthquake relocation with improved travel times and procedures for depth determination, *Bull. Siesm. Soc. Am.*, v.88, pp. 722-743.
3. Ge, M. (1995). Comment on "Microearthquake location: a non-linear approach that makes use of a Simplex stepping procedure" by A. Prugger and D. Gendzwell, *Bull. Seism. Soc. Am.* 85, pp. 375-377.
4. Geiger, L. (1912). Probability method for the determination of earthquake epicentres from the arrival time only, *Bull. St. Louis. Univ.* 8, pp. 60-71.

5. Gendzwil, D. and A. Prugger (1989). Algorithms for micro-earthquake location, in *Proc. 4th Conf. Acoustic emission/Microseismic Activity in Geologic Structures, Trans Tech. Publications, Clausthal-Zellerfeld, Germany*, 601-605.
6. *Global Seismograph Network – IRIS/IDA* // International Federation of Digital Seismograph Networks [Site]. – DOI: 10.7914/SN/II (date of request 23.01.2024).
7. *Global Seismograph Network (GSN – IRIS/USGS)* // International Federation of Digital Seismograph Networks [Site]. – DOI: 10.7914/SN/IU (date of request 23.01.2024).
8. Murphy, J.R. & Barker, B.W., (2006). Improved focal-depth determination through automated determination of seismic depth phases pP and sP, *Bull. Seism. Soc. Am.*, v.96, 1213-1229.
9. William T. Vetterling, Brian P. Flannery, William H. Press, Saul Teukolsky, (1988) *Numerical Recipes, The Art of Scientific Computing*, Cambridge University Press, pp. 818.
10. Prugger, A. and D. Gendzwil (1989). Micro-earthquake location: a non-linear approach that makes use of a Simplex stepping procedure, *Bull. Seism. Soc. Am.* 78, pp. 799-815
11. Dmitry Storck, (2011). Improved location procedures at the International Seismological Centre, *Geophysical Journal International*, 186, pp. 1220-1244.

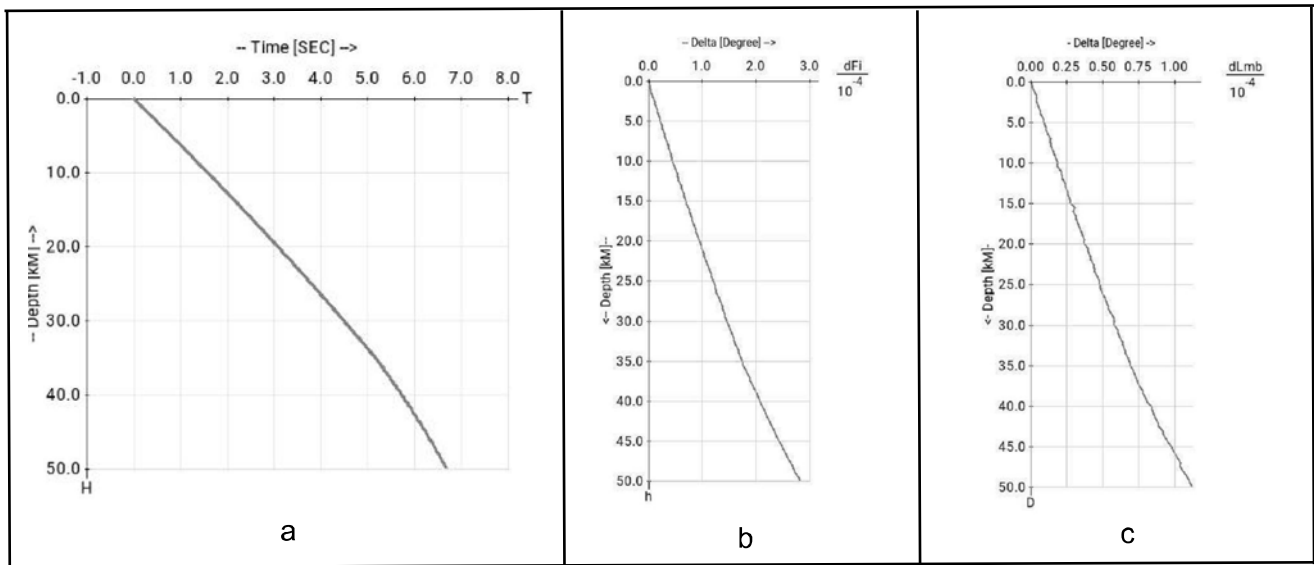


Fig. 1: Rupture line example for event 2022-01-07 17:45:34 in China. This is not a real rupture on this line, this is the geometrical places (locus) hypocentre coordinates in dependence of depth. Each hypocentre is calculated for a fixed depth. Each coordinate (except depth) is plotted as a difference of its value on depth and its value on the zero depth: (a) - origin time coordinate values, (b) - latitude values, (c) - longitude values. Depth range – from zero up to 50km.

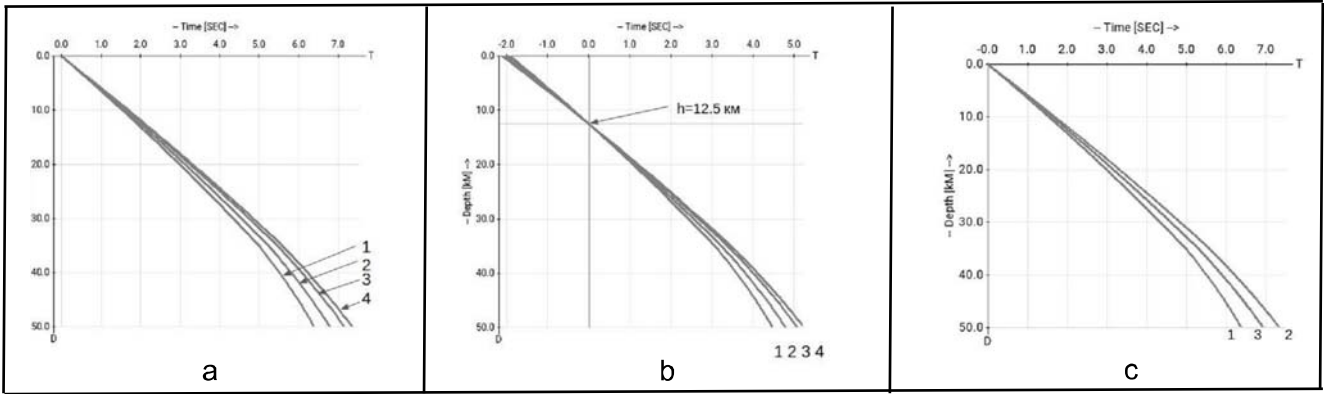


Fig. 2: Examples of graphs of P characteristics origin time $t_0^x(r, h)$ and rupture line origin time $t_0^y(h)$. Plot (a) presents four graphs of $t_0^x(r, h)$ at four epicentral distances: (1) $r = 25 \text{ degr.}$, (2) $r = 50 \text{ degr.}$, (3) $r = 75 \text{ degr.}$, (4) $r = 100 \text{ degr.}$ and focus depth $h^f = 0.0 \text{ km}$. Plot (b) presents four graphs of $t_0^x(r, h)$ at four epicentral distances as it was on plot (a), but for focus depth $h^f = 12.5 \text{ km}$. Last plot (c) presents two P characteristics origin times $t_0^x(r, h)$ at the distances: $r = 25 \text{ degr.}$ line 1, $r = 100 \text{ degr.}$ line 2, and graph of origin time of the rupture line 3. The rupture line is the processing results of the event 2022-01-07 17:45:34 in China. (h^f is some fixed depth).

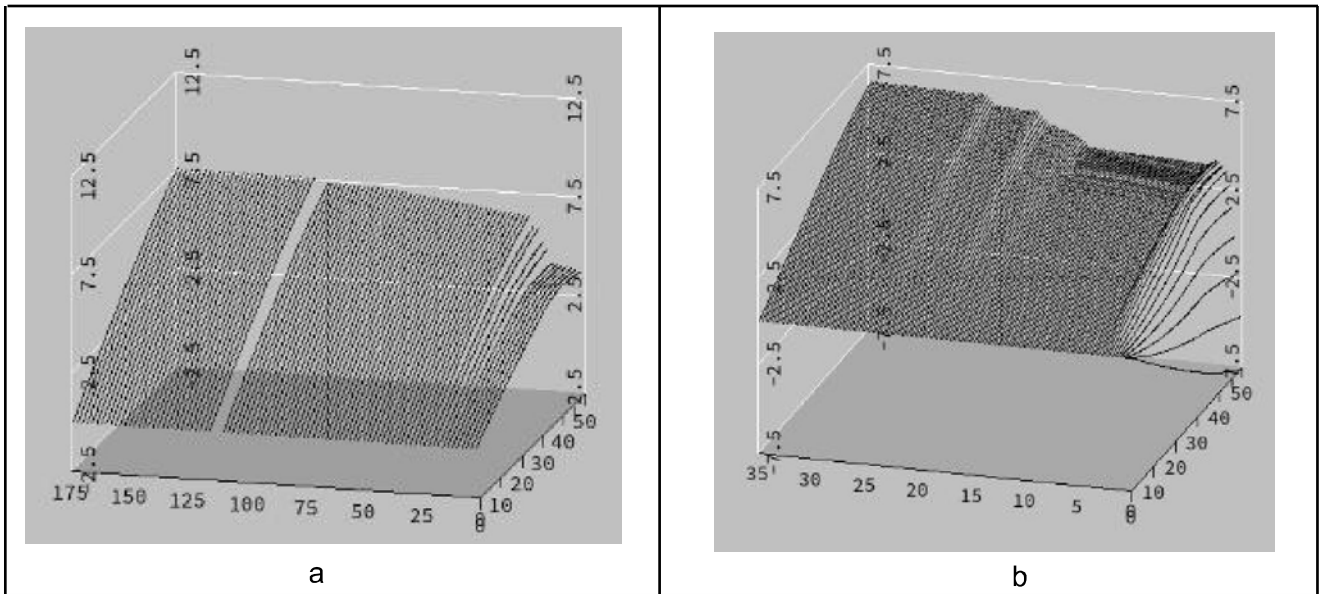


Fig. 3: 3D projection of two dimensional function $t(r, h) = (\gamma^P(r, h) - \gamma^P(r, 0))$ which is a difference of $t_m^0(r, h)$ and $t_m(r, h)_{h=0}$, where $m =$ index over epicentral distances. The plot is drawn for argument value intervals: a - $r = (2, \dots, 175)^\circ$, $h = (0, \dots, 50) \text{ km}$, b - $r = (0, \dots, 35)^\circ$, $h = (0, \dots, 50) \text{ km}$. There are easy to see different zones distributed by epicentral distances: first - local zone, second - regional zone, third - transmission zone and fourth - teleseismic zone. The travel time table for the P phase has one degree gap.

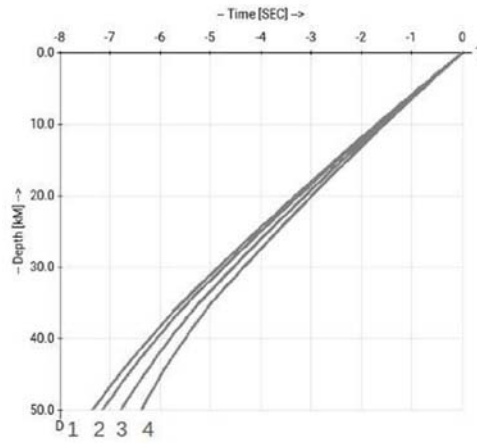


Fig. 4: Examples of graphs of pP characteristics origin time $t_0^x(r, h)$. Epicentral distances are the same as on fig. 2.

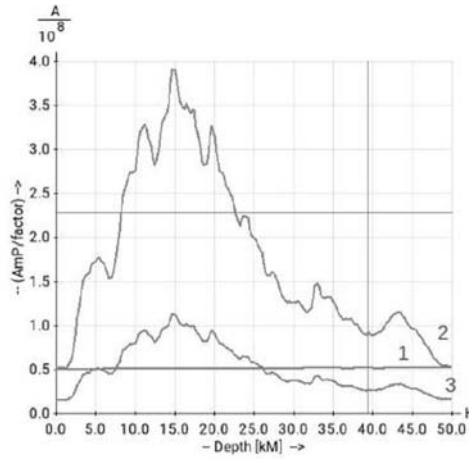


Fig. 5: Example of location data processing of the event 2022-01-07 17:45:34 in China. This presents two graphs of values of the amplitude parameters : 1- phase P , 2- phase pP ; third graph plotted for value obtained by expression (9) – first algorithm of amplitude coordinations.

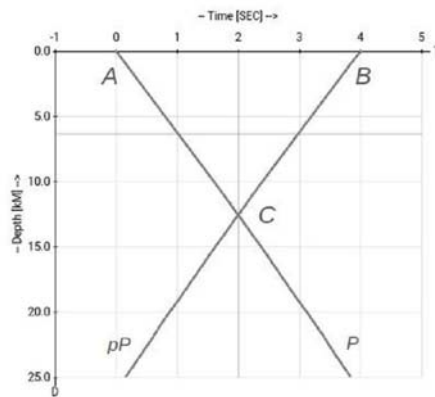


Fig. 6: Schematic chart of collaborations of pairs of the seismic phases: points A and B are situated on the time axis, segments (A, C) and (B, C) and its continuations are characteristics. The consideration is in the text.

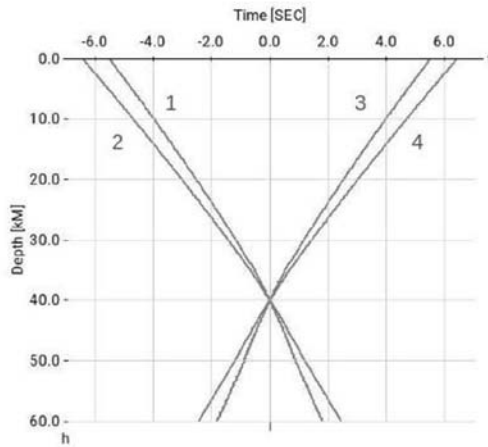


Fig. 7: Deviations of time at the crossing points of P and pP characteristics due to epicentral distances. 1- P characteristic for $r = 25^\circ$, 2 - P characteristic for $r = 175^\circ$, 3 - pP characteristic for $r = 25^\circ$, 4 - pP characteristic for $r = 175^\circ$. Zero on time axis corresponds to origin time, values on time axis are differences between phase origin time on depth zero and $t_0^{wv}(h)_{h=h^f}$ which is the origin time on the rupture line. Crossing point corresponds to depth $h^f = 40.0 \text{ km}$.

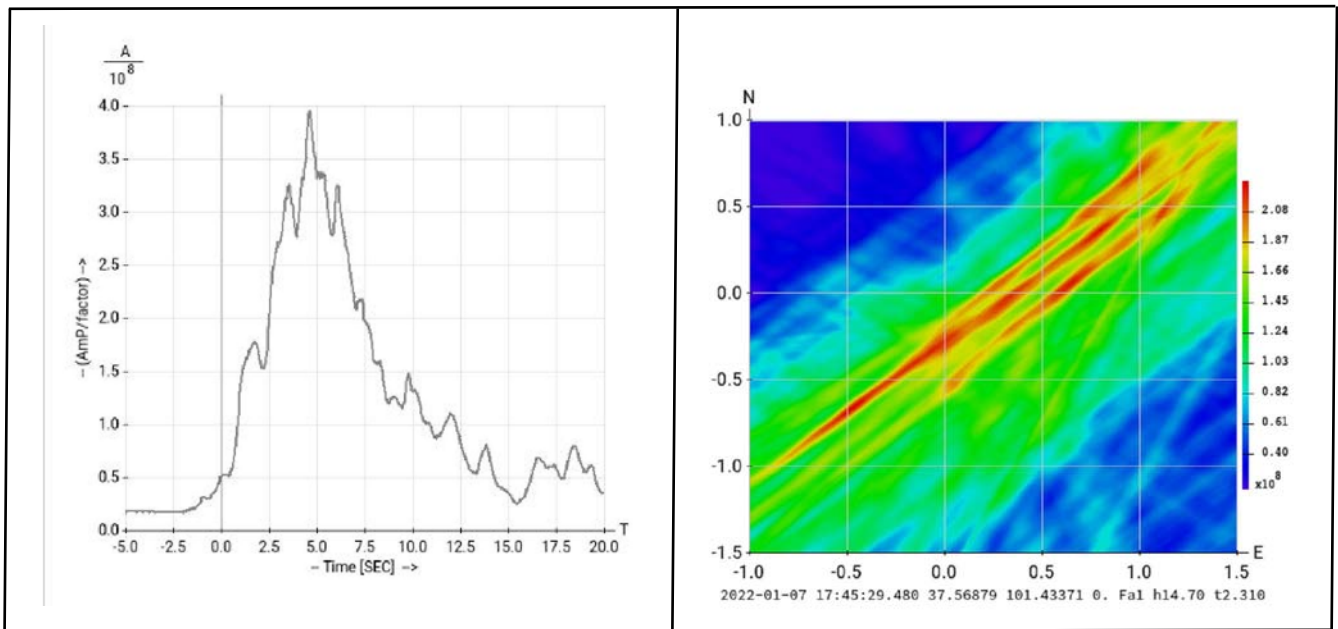


Fig. 8: (left) Graph of the generalized AmP parameter obtained from data processing of event 2022-01-07 17:45:34 in China. The time interval $t = (-5, \dots, 20) \text{ sec}$; zero of the time axis corresponds to $t_0^{wv}(h)_{h=0}$.

Fig. 9: (right) Map of seismic activity at the depth of origin $n = 14.7 \text{ km}$. Units along the axis are arc degrees.

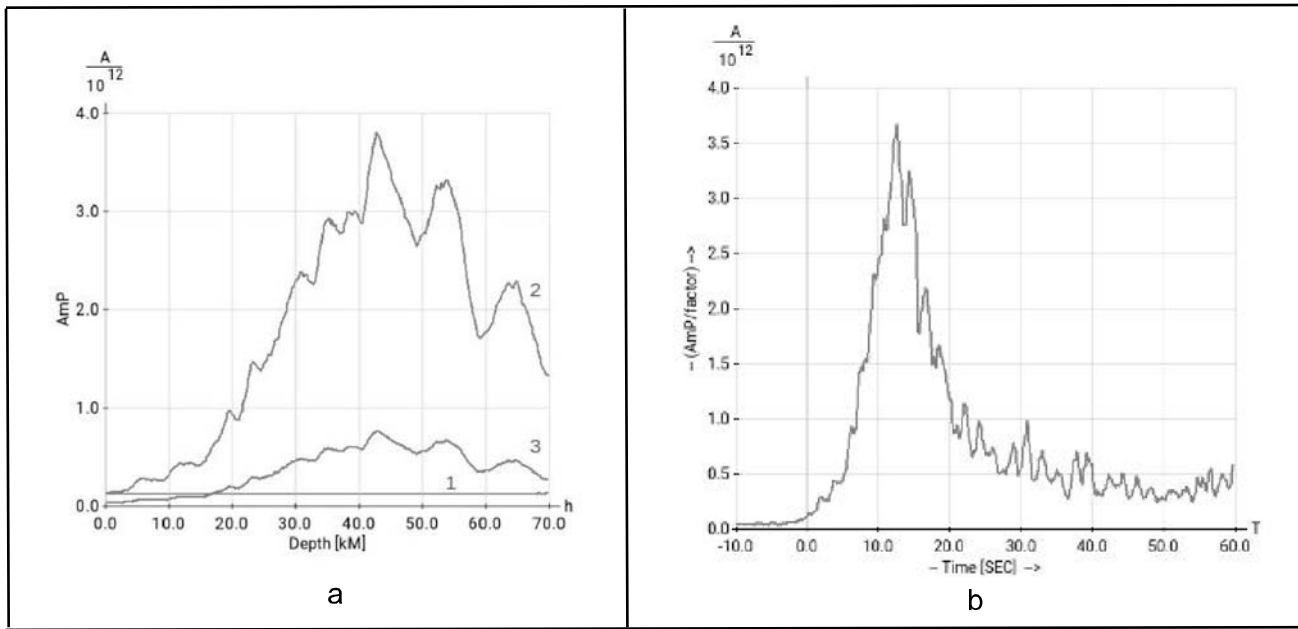
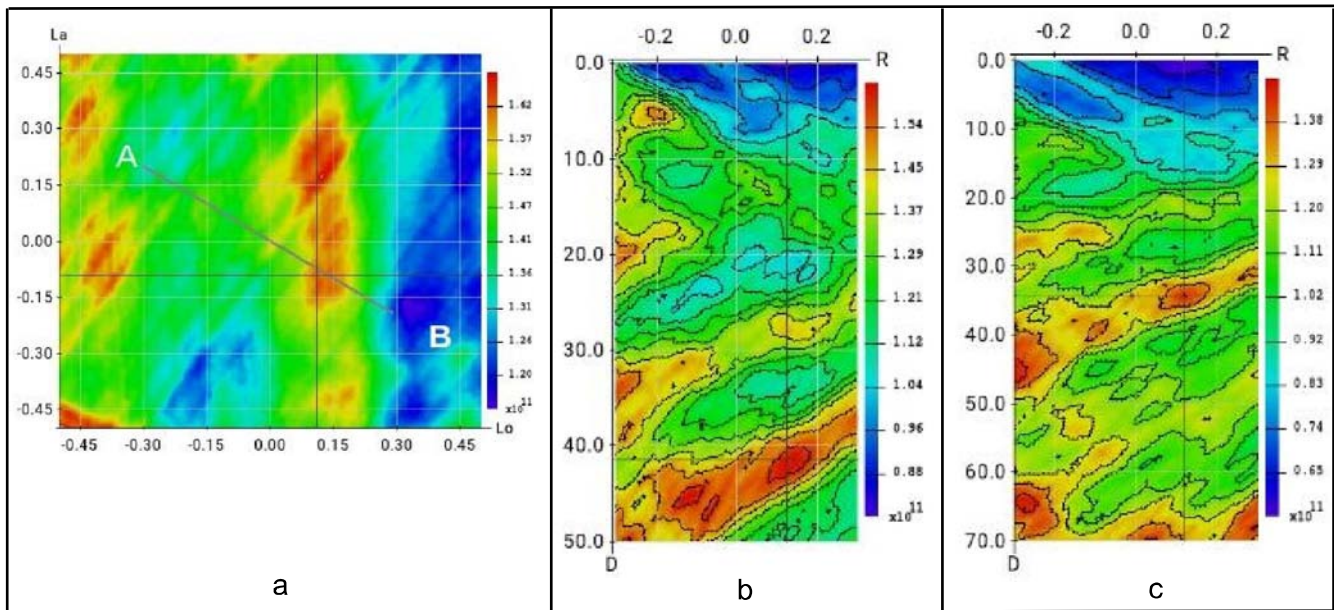


Fig. 10: Example of the results of location data processing of the event 2024-01-22 18:09:09 border of Kyrgyzstan and China: a- three graph which are used for depth determination: line (1) parameter $AmP^P(\mathcal{W})$, line (2) parameter $AmP^{PP}(\mathcal{W})$, line (3) $A_k - (pP \text{ to } P)$ - -translated parameter(9); b- graph of the averaged AmP parameter in time interval $t = (-10, \dots, 60)$ sec; zero of the time axis corresponds to $t_0^{\mathcal{W}}(h)_{h=0}$.



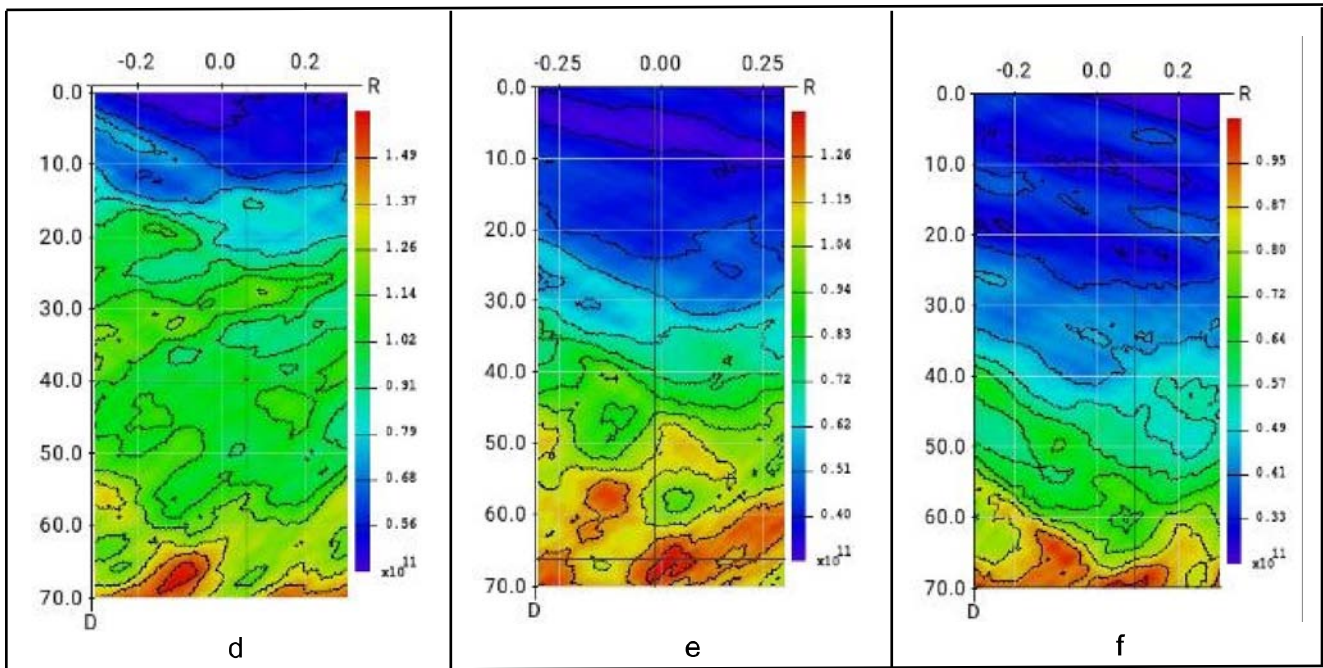


Fig. 11: Examples of focus zone interior analysis; event 2024-01-22 18:09:09 border of Kyrgyzstan and China: map of seismic activity on the origin depth (a), and series of the vertical slices hose horizontal cut given on map (a) as a (A, B) line; series presented for times: b- $t_p = 0 \text{ sec}$, c- $t_p = -1 \text{ sec}$, d - $t_p = -2 \text{ sec}$ and e - $t_p = -5 \text{ sec}$, f - $t_p = -7.5 \text{ sec}$, where t_p precursor time before $t_0^{W_{h=0}}$. Time corresponds to the time axis on Fig.10.b. These figures were plotted by using the (11) algorithm of amplitude coordinations.